Supplementary Material

Photocatalytic reactions of a Nickel(II) annulene complex incorporated in polymeric structures.

G. Estiu, G. Ferraudi, A. G. Lappin, G. T. Ruiz, C. Vericat, J. Costamagna, M. Villagran

General methods and techniques.

TEM and AFM methodologies. These microscopies were used to investigate the morphologies of the polymer in various medium conditions. To prepare samples for transmission electron microscopy (TEM), a drop of the sample solution was placed on a Formvar coated copper grid, stabilized with a carbon film. It was kept on the grid 5 min and the excess liquid was then removed by placing the grid on a filter paper. Transmission electron micrographs were recorded on a Philips EM 301 electron microscope at an electron acceleration voltage of 60 kV. Stock solutions of the poly(Ni^{II}[tmdbzTAA])$_1$ were prepared by dissolving the polymer in water at pH = 10 or acetonitrile and diluting them as necessary for the preparation of the sample solutions.

Atomic Force Microscopy (AFM) imaging was performed in air in the Tapping^{TM} mode with a Multimode microscope commanded by a Nanoscope V control unit, both from Veeco Instruments (Santa Barbara, CA, USA). Silicon probes (f_o = 285 kHz; k = 42 N/m) from NanoWorld (Switzerland) were used in all measurements. Samples were prepared by drop-casting the polymer solutions on freshly cleaved muscovite mica (Ted Pella Inc, USA).

Cyclic voltammetry. Cyclic Voltammetry measurements were performed on a potentiostate/galvanostat PAR-173, Universal Programmer PAR-175, and a digital Coulometer PAR-179 from Princeton Applied Research. An H cell with three electrodes, namely glassy carbon, platinum wire, and saturated calomel electrode (SCE), as working, auxiliary, and reference electrodes, respectively, was used. The solvent and the supporting electrolytes were DMF and tetraethylammonium perchlorate (TEAP), respectively. All measurements were carried out under nitrogen atmosphere at 25 °C.

Cyclic voltammetry measurements were used in a time-resolved study of the [Ni^{II}(tmdbzTAA-CO- - -)] protonation process followed by cyclic voltammetry. In these experiments, a Pt disk, a Pt wire and a saturated calomel electrode were used in that order as working, auxiliary and reference electrodes. The working electrode was cleansed after each sweep to eliminate any possible contamination such as the formation of polymer films on the electrode surface.

Spectroscopic measurements. UV-Vis-NIR spectra were recorded with a Shimadzu UV-3101PC and -1800 spectrophotometers. FTIR spectra were recorded with a Bio-Rad FTS 175 Spectrometer. The steady state luminescence of the polymers was studied with a Fluorolog spectrofluorimeter. NMR spectra were recorded with solutions deaerated with streams of N_2 or Ar gas. ^{1}H-NMR spectra were recorded from deuterated dimethylsulfoxide solution of the compounds at 300 K on a Bruker Avance 400 spectrometer operating at 400.13 MHz, and equipped with a 5 mm broadband inverse probe head incorporating a z-gradient coil. The chemical shift (ppm) are reported relative to tetramethylsilane and calibrated with respect to residual solvent protons.

Flash photochemical procedures. Absorbance changes, ΔA, occurring in a time scale longer than 10 ns were investigated with a flash photolysis apparatus described elsewhere. [7] In these experiments, 10 ns flashes of 351 nm light were generated with a Lambda Physik SLL -200 excimer laser. The energy of the laser flash was attenuated to values equal to or less than 20 mJ/pulse by absorbing some of the laser light in a filter solution of $Ni(ClO_4)_2$ having the desired optical transmittance, $T = I_t / I_0$ where I_0 and I_t are respectively the intensities of the light arriving to and transmitted from the filter solution. The transmittance, $T = 10^{-A}$, was routinely calculated by using the spectrophotometrically measured absorbance, A, of the filter solution. A right angle configuration was used for the pump and the probe beams. Concentrations of poly(Ni^{II}[tmdbzTAA])$_n$ compounds were adjusted to provide homogeneous concentrations of photogenerated intermediates over the optical path, l = 1 cm, of the probe beam. To satisfy this optical condition, solutions were made with an absorbance equal to or less than 0.8 over the 0.2 cm optical path of the pump. Unless explicitly stated, aqueous solutions of poly(Ni^{II}[tmdbzTAA])$_n$ were buffered either with borate-boric acid buffer at pH = 8, phosphate buffer at pH = 6 and borate-KOH buffer at pH = 10 in the photochemical studies.

The reaction kinetics were investigated by following the absorbance change at given wavelengths of the spectrum and incorporating those changes in the dimensionless parameter, $\xi = (\Delta A_{inf} - \Delta A_t)/(\Delta A_{inf} - \Delta A_0)$. [8] In ξ, ΔA_0 is the absorbance change at the beginning of the reaction, ΔA_t is determined at an instant t of the reaction and ΔA_{inf} is determined at the end of the reaction.

Time-resolved fluorescence experiments were carried out with the flash photolysis apparatus described above. The 532 nm excitation light was provided by the Nd YAG laser. All the solutions used in the photochemical work were deaerated 30 min with streams of ultrahigh-purity N_2 before and during the irradiations.

Steady state photolysis procedures. The collimated light of a 1KW Xe lamp was passed through 10 cm of distilled water and a cut-off filter transmitting only wavelengths of the light longer than 400 nm. A Bausch & Lomb monochromator replaced the cut-off filter for the monochromatic 520 nm and 365 nm irradiations of poly(Ni^{II}[tmdbzTAA])$_n$ solutions. The half-height bandwidth of the quasi monochromatic light was ~5 nm. Actinometric measurements gave a 10^{-4} Einstein L^{-1} min^{-1} order of magnitude for the light intensity at 365 nm and 532 nm. The Reineke salt actinometer was used for the determination of the 520 nm light intensity. [9]

CO and SO_4^{2-} analyses. Irradiated solutions of poly(Ni^{II}[tmdbzTAA])$_n$ solutions were frozen to $N_2(l)$ temperature. Samples of the photolysis products not frozen solid at this temperature: H_2, CO and CH_4 were transferred with the Toepler pump technique to a Shimadzu GC-17A gas chromatograph equipped with a molecular sieves column and a TC detector. Samples of the pure gasses were

used for the calibration of the gas chromatograph. Blanks were made with solutions of the same composition of the irradiated solutions but kept in the dark for periods equal to those used in the irradiations.

The formation of the S(VI) photoproducts, e.g., HSO_4^- and SO_4^{2-}, was qualitatively investigated with BaCl. A photolyzed solution was boiled to near dryness to eliminate SO_2 and CO_2 and warmed to ~50°C after the addition of 20 mL of 0.01 M HCl. The subsequent addition of a concentrated solution of $BaCl_2$ in 0.01 M HCl produced a precipitate of $BaSO_4$. Analyses made with unirradiated solutions of poly(Ni^{II}[tmdbzTAA])$_n$ produced no precipitates.

Pulse-Radiolytic Procedures. Pulse radiolysis experiments were carried out with a model TB-8/16-1S electron linear accelerator following previously described methods. [10] The instrument and computerized data collection for time-resolved UV-Vis spectroscopy and reaction kinetics have been described elsewhere in the literature. [11]Thiocyanate dosimetry was carried out at the beginning of each experimental session. The details of the dosimetry have been reported elsewhere . [11, 12]The procedure is based on the concentration of $(SCN)_2^{\bullet-}$ radicals generated by the electron pulse in a N_2O saturated 10^{-2} M SCN^- solution. In the procedure, the calculations were made with G = 6.13 and an extinction coefficient, $\varepsilon = 7.58 \times 10^3$ $M^{-1}.cm^{-1}$ at 472 nm, for the $(SCN)_2^{\bullet-}$ radicals. [12] In general, the experiments were carried out with doses that in N_2 saturated aqueous solutions resulted in $(2.0\pm0.1) \times 10^{-6}$ M to $(6.0\pm0.3) \times 10^{-6}$ M concentrations of e^-_{sol}. In these experiments, solutions were deaerated with streams of the O_2-free gas, N_2 or N_2O, that was required for the experiment. Reactions of the radiolytically generated $OH^\bullet$ radicals HCO_2^- or 2-propanol were used for the preparation of the reactive radicals $CO_2^{\bullet-}$ and $(CH_3)_2COHC^\bullet H_2$, Scheme SI. Other experiments, where the simultaneous generation of $(CH_3)_2COHC^\bullet H_2$ and e^-_{sol} was desired, were conducted with N_2-deaerated solutions containing 0.1 M $(CH_3)_3COH$ as a scavenger of the radiolytically generated $OH^\bullet$ radicals.

In order to radiolyze a fresh sample with each radiolytic pulse, an appropriate flow of the solution through the reaction cell was maintained during the experiment. Aqueous solutions of poly(Ni^{II}[tmdbzTAA])$_n$ were buffered either with borate-boric acid

$$RH = HCO_2^-, N_3^-, CH_3OH, (CH_3)_2COH \; ;$$
$$R^\bullet = CO_2^{\bullet-}, N_3^\bullet, C^\bullet H_2OH, (CH_3)_2C^\bullet OH$$
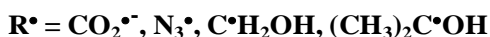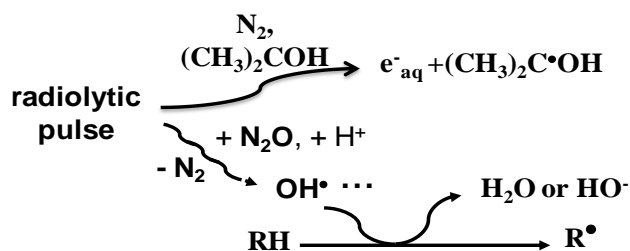
buffer at pH = 8 or phosphate buffer at pH = 6. Other conditions used for the time-resolved spectroscopy of the reaction intermediates or in the investigation of the reaction kinetics are given in the Results section.

Computational Methods. The density functional theory (DFT) methods implemented in Gaussian 09 [13] have been used to analyze the structure and better assign the nature of the intermediates resulting from the pulse radiolysis experiments. This has been done through calculation of the UV-Vis spectra for different possible models, choosing the one that best reproduces the experimental features. As the transitions are centered in the pendant, a model has been used that includes the Ni-annulene pendant and a 6-acetyl capping group.

The systems studied herein were subjected to unrestrained energy minimizations using the B3LYP functional [14 -18] with the 6-31+G* basis set [19] for nonmetal atoms and the Los Alamos effective core potentials (LANL2DZ) [20] for the metal. The solvent has been modeled within a continuous approach (Polarizable Continuous Model, PCM) [21] and time dependent DFT models were used to assign the nature of the observed electronic transitions in the UV-vis spectra.

The extended systems were also modeled using small polymer strands (6 units), running short molecular dynamics simulations (MD) using the OPLS force field and Macromodel [22] software (Schrodinger). Different protonation states of the carboxylate groups were considered in order to visualize potential interactions that may contribute to stabilize the strands.

Structural and Morphological study of poly(Ni^{II}[tmdbzTAA])$_n$.

In contrast to Ni^{II}[tmdbzTAA], the polymeric materials, poly(Ni^{II}[tmdbzTAA])$_n$, n = 1,2, exhibit good solubility in water at pH ≥ 6, up to 200 mg in 100 cm^3, and they precipitate when the solutions are acidified to pH ≤ 6. In the protonated form produced at pH< 6, the polymers can be dissolved in polar organic solvents such as CH_3CN. Given this range of properties, TEM and AFM techniques were used to investigate the morphology of poly(Ni^{II}[tmdbzTAA])$_2$ in the solid state and solution phase. Solutions of poly(Ni^{II}[tmdbzTAA])$_1$ in CH_3CN containing concentrations of $HClO_4$ ranging from 0.01 to 0.1 M were used for the TEM observations. In these solutions, the polymer appears as stick-like structures with some of them showing some roundels or spherules, Fig. S3. The elongated shapes were also observed in AFM micrographs of preparations made with diluted solutions of poly(Ni^{II}[tmdbzTAA])$_1$, ~ 2 mg in 25 cm^3, in CH_3CN containing between 0.1 and 0.01 M of $HClO_4$. Nearly the same shapes were observed in the TEM, and AFM. Nevertheless, the shapes seen in both microscopies are too thick to correspond to a single polymer strand and must be r concentrations of $HClO_4$ ranging from 0.01 to 0.1 M were used for the TEM observations. In these solutions, the polymer appears as stick-like structures with some of them showing some roundels or spherules, Fig. S3, regarded as bundles of polymer strands.

When using aqueous solutions, the pH was adjusted to values between 8 and 10 with NaOH. Globular shapes, shown in Fig. S4a, were observed in AFM micrographs corresponding to preparations made with the most concentrated solutions. In contrast to the globular shapes, elongated and contorted morphologies were observed when the preparations were made with diluted solutions of poly(Ni^{II}[tmdbzTAA])$_1$, Fig. S4b. Elongated shapes, similar to those seen in Fig. 2b, were observed in TEM micrographs of preparations made with diluted solutions of poly(Ni^{II}[tmdbzTAA])$_1$, Fig. S4c. A comparison of the TEM and AFM experimental observations suggest that bundles of polymer strands have coiled

structures which in some case may approach an helix and in all cases depart from the linear shapes seen in the CH$_3$CN preparations.
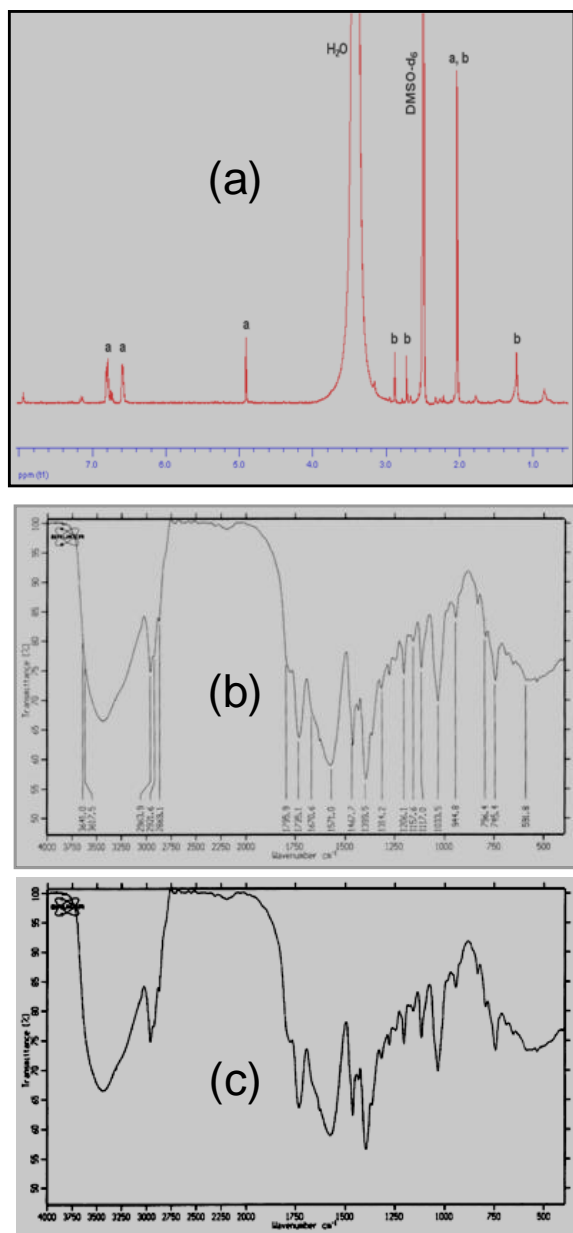
Figure S1. Spectroscopic properties of poly(Ni[tmdbzTAA])₂. (a): NMR spectrum in dimethylsulfoxide–d₆ and (b) and (c): FTIR in solid phase.
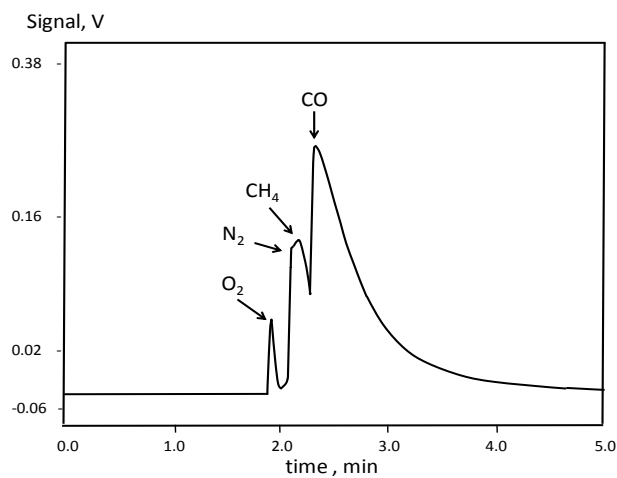

Figure S2. Typical GC chromathogram recorded with the gas collected from an aqueous solution of poly(Ni[tmdbzTAA])₂ saturated under 1 atm with a 1:1 molar mixture of CO_2 and SO_2. The gas sample was collected after a 24 h photolysis of the solution at 365 nm. Labels in the figure identified the components of the gas sample. Additional experimental details are given in the text.
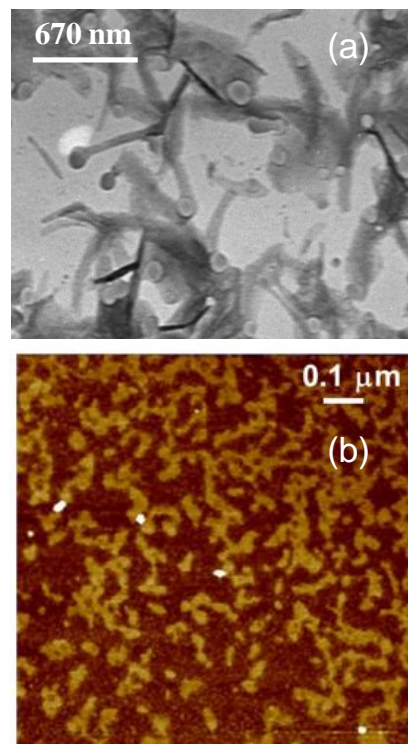
Figure S3. TEM microgrph (top) recorded with poly(Ni^{II}[tmdbzTAA])₂ solutions containing 0.1 and 0.01 M $HClO_4$ in CH_3CN. AFM micrograph of the polymer (bottom). Sample prepared from an acidic solution of the polymer in CH_3CN. Z scale: 5 nm.
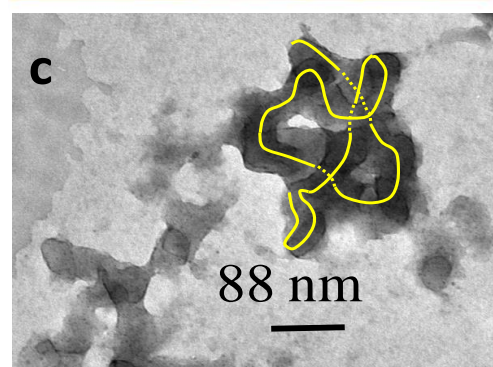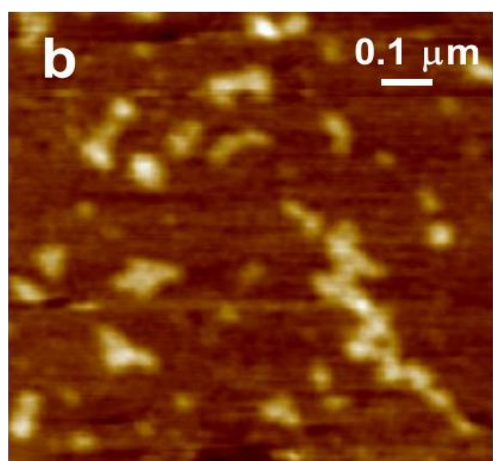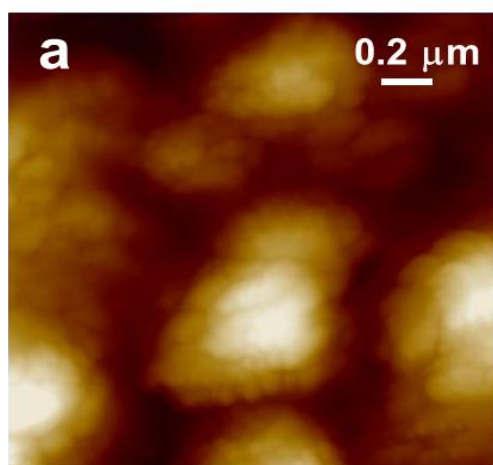
Figure S5. Cathodic (a) and anodic (b) voltammetric responses of poly(Ni[TMBzTAA])$_2$ in N,N'-dimethylformamide with NH$_4$ClO$_4$ support electrolyte. Other experimental details are communicated in the text.

Figure S4. Structures of poly(Ni^{II}[tmdbzTAA])$_1$ observed with the AFM in basic solution: (a) concentrated, (b) diluted. Z scale: (a) 300 nm, (b): 3 nm. (c) TEM structures from basic solutions. A yellow line has been inserted to highlight the shape o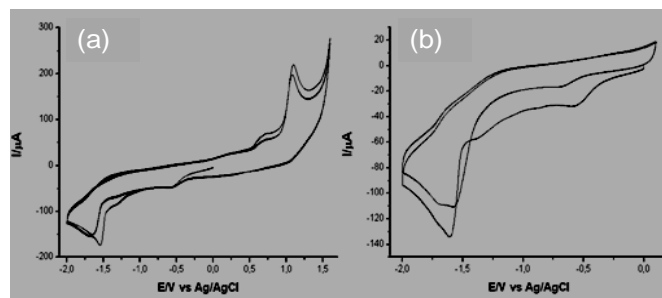f the bundle. Scales are indicated in the figure.